result, average degradation rates over complete pulses increased with the mean rate of change of applied heating. Average measured surface recession rates were approximately constant, however.

The experimental transient heating ablation measurements were compared with calculated response based on steady-state heating test results. For minimum and maximum rates of change of applied heating, respectively, the measured degradation was ~15% less to 30% more than calculated over complete pulses, and 7% to 36% more than calculated during increasing heating. The corresponding measured surface recession measurements were approximately 10% more to 7% less than calculated over complete pulses, and 15% more to 10% less than calculated for increasing heating. These results indicate that the analytical procedures used in transient heating ablation cases should include analyses of the mechanism producing the transient effects.

## References

[1] Strouhal, G., Curry, D. M., and Janney, J. M., "Thermal Protection System Performance of the Apollo Command Module," *AIAA/ASME 7th Structures and Materials Conference*, AIAA, New York, 1966, pp. 194–200.

[2] Brunner, M. J., Dolan, C., Grasier, R., Kottock, S., Merlo, G., "Study of Thermal Protection Requirements for a Lifting Body Entry Vehicle Suitable for Near-Earth Missions," Document No. 66SD253, May 12, 1966, General Electric Co., Philadelphia, Pa. (Final Report, NASA Contract NAS-2-2974).

[3] Hiester, N. K., Clark, C. F., and Vojvodich, N. S., "Ablative Characterization of Seven Heat Shield Materials—A Review of the NASA-SRI Round-Robin Program," *AIAA/ASME 10th Structures, Structural Dynamics and Materials Conference*, AIAA, New York, 1969, pp. 57–68.

[4] Gowen, F. E., and Nichols, F. H., "The Ames Combined Heating Facility," AIAA Paper 69-342, Cincinnati, Ohio, 1969.

[5] Lundell, J. H., Winovich, W., and Wakefield, R. M., "Simulation of Convective and Radiative Entry Heating," Symposium on Hypervelocity Technique, Denver, Colo., March 20–21, 1962.

[6] Shepard, C. E. and Winovich, W., "Electric-Arc Jets for Producing Gas Streams with Negligible Contamination," Paper 61-WA-247, American Society of Mechanical Engineers.

[7] Lundell, J. H., Wakefield, R. M., and Jones, J. W., "Experimental Investigation of a Charring Ablative Material Exposed to Combined Convective and Radiative Heating," *AIAA Journal*, Vol. 3, No. 11, Nov. 1965, pp. 2087–2095.

[8] Lundell, J. H., Dickey, R. R., and Jones, J. W., "Performance of Charring Ablative Materials in the Diffusion Controlled Combustion Regime," *AIAA Journal*, Vol. 6, No. 6, June, 1968, pp. 1118–1126.

[9] Wakefield, R. M., Lundell, J. H., and Dickey, R. R., "Effects of Pyrolysis-Gas Chemical Reactions on Surface Recession of Charring Ablators," *Journal of Spacecraft and Rockets*, Vol. 6, No. 2, Feb. 1969, pp. 122–128.

JUNE 1971 J. SPACECRAFT VOL. 8, NO. 6

# Heating Environment and Protection during Jupiter Entry

MICHAEL E. TAUBER* AND ROY M. WAKEFIELD†
*NASA Ames Research Center, Moffett Field, Calif.*

**The heating-rate histories and heat-shielding requirements for three different-sized Jupiter atmospheric probes, designed to survive entry, are studied parametrically. Atmospheres varying from 60% hydrogen-40% helium to pure hydrogen are considered. Recently, more sophisticated calculations of radiative absorption by ablation-product vapors have revealed large heating reductions at the body surface for steep Jovian entries. If up to half the probe's weight is devoted to heat protection, then steep, as well as shallow, angle entries appear feasible, assuming a graphite-class heat shield can function reliably at heating rates on the order of 100 kw/cm².**

## Nomenclature

$A$ = base area of entry body, m²
$C_D$ = drag coefficient
$m$ = vehicle mass at any time $t$, kg
$\dot{m}$ = surface mass-loss rate per unit area, kg/m² sec
$m_E$ = body mass at entry, kg
$m_H$ = heat-shield mass; $\Delta m_H$ ablated mass, kg
$p_2$ = shock-layer pressure, atm
$\dot{q}$ = heat-transfer rate, kw/cm²
$\dot{q}_R$ = radiative-heat-transfer rate; $\dot{q}_{R_{AD}}$ value for adiabatic shock layer
$r_b$ = base radius of body, m
$Re_{BT}$ = local Reynolds number for beginning of transition
$t$ = time, sec
$V_r$ = velocity with respect to rotating atmosphere, m/sec
$\gamma_{IE}$ = inertial coordinate entry path angle, deg
$\Gamma$ = radiative cooling parameter
$\delta_{AD}$ = adiabatic shock-layer thickness
$\theta_c$ = cone half-angle, deg
$\theta_s$ = cone shock-wave angle, deg
$\rho$ = atmospheric density, kg/m³

Presented as Paper 70-1324 at the AIAA 7th Annual Meeting and Technical Display, Houston, Texas, October 19–22, 1970; submitted October 19, 1970; revision received March 1, 1971.

* Research Scientist, Hypersonic Free-Flight Branch, Vehicle Environment Division. Associate Fellow AIAA.

† Research Scientist, Thermal Protection Branch, Thermo- and Gas-Dynamics Division.

## Introduction

THE velocity of entry into the Jovian atmosphere will exceed 60 km/sec. A previous paper[1] showed that heat-shield ablation might be kept within tolerable limits by making near equatorial posigrade entries (i.e. in the direction of planetary rotation) at very shallow flight-path angles, holding Reynolds numbers below selected values to avoid transition to turbulent flow (assumed to be intolerable). Four atmospheric compositions ranging from pure hydrogen to pure helium were considered, and combinations of bodies and trajectories which could succeed for all atmospheric compositions were found. The design in such a case, where atmospheric composition is unknown, must be a compromise of the optimum designs for each specific atmosphere. In

**Table 1 Atmospheres considered**

| Composition mole % | Molecular weight | Scale height, km |
|---|---|---|
| 60 $H_2$–40 He | 2.80 | 17.0 |
| 85 $H_2$–15 He | 2.30 | 20.7 |
| Pure $H_2$ | 2.00 | 23.8 |

addition to posing guidance difficulties, the very shallow flight-path angles limited the entries to the night side of the equatorial region, thus imposing restraints on the scientific objectives and communication aspects.

Boundary-layer transition to turbulence is permitted in this paper and the equatorial and polar entries of a number of specific bodies are investigated. Also, only hydrogen-rich atmospheres (Table 1) are considered because of more recent information on the composition of the Jovian atmosphere.[2–4] A constant stratospheric temperature of 140°K has been assumed. A pure hydrogen atmosphere is included as a limiting case although this composition is probably unrealistic.

Three size and weight combinations of entry probes are considered (Table 2). All are assumed to have conical forebodies with small initial nose blunting. Cone angles and, consequently, ballistic coefficients are determined from the analysis. The maximum body weight of 500 kg represents, roughly, the maximum entry vehicle payload capacity of the Jet Propulsion Laboratory (JPL) TOPS (thermoelectric outer planetary spacecraft). The 100 kg body is thought to be near the smallest practicable, or feasible for multiprobe missions. The 250 kg body is the nominal case and represents the approximate entry vehicle payload of a Pioneer spacecraft.

Ablation vapor blockage of radiative heating is accounted for in this study and the results of radiative cooling calculations in hydrogen-helium mixtures are used (cooling results for air were used in Ref. 1). Although the basic ablator behavior simplification of Ref. 1 has been retained, it is now based on more rigorous calculations in the Jupiter atmospheric environment; in addition, heat-shield insulation requirements are estimated. Such potential problems of heat-shield-material response (especially during steep entries) as particulate removal and thermal stress failure cannot yet be reliably assessed. Many of the detailed calculations of the heating environment and material response are at the border of the present state-of-the-art or beyond.

## Analysis

### Radiative Heating

The heating of the bodies, with cone angles in the neighborhood of the optimum is dominated by shock-layer radiation. Fortunately, natural physical mechanisms (nonadiabatic effects) exist for reducing the emission substantially below the value of an adiabatic shock layer. This so-called radiative cooling effect is illustrated in Fig. 1, where the reduction in radiation due to the nonadiabatic shock layer is shown as a function of the radiation cooling parameter, defined as

$$\Gamma = 4\dot{q}_{R_{AD}}/\rho V_r^3$$

for a stagnation-point flow, or

$$\Gamma = 4\dot{q}_{R_{AD}}/\rho V_r^3 \sin^3\theta_s$$

for a cone. Shown in Fig. 1 is a band of calculations for air (based on Ref. 5); in addition, eight individual values for realistic flight conditions were computed for two hydrogen-helium mixtures by K. H. Wilson of Lockheed under contract to Ames Research Center. Although the cooling appears to be somewhat less pronounced than in air, the general trend is similar. The product of adiabatic shock standoff distance and shock-layer pressure, which is a rough measure of the optical depth, was varied over two orders of magnitude (as opposed to a factor of 3 for the air band) and one curve was fitted through the calculated values (guided by the air curve) and used for the hydrogen-helium atmospheres considered. The expression used, which is shown by the dashed line in Fig. 1, is (for $\Gamma < 1$)

$$(\dot{q}_R/\dot{q}_{R_{AD}})_{\dot{m}=0} = 1/(1 + 3\Gamma^{0.7})$$

The rationale for using one expression for both atmospheres is that the variation of cooling between atmospheres is on the same order as that due to changing optical depth and that both are probably within the uncertainty of other simplifying assumptions made in the analysis, such as applying the stagnation-point results of Fig. 1 to the flank of a cone. (For an optically thin gas, the last assumption is reasonable, according to Ref. 6, for the range of $\Gamma$ of interest here.)

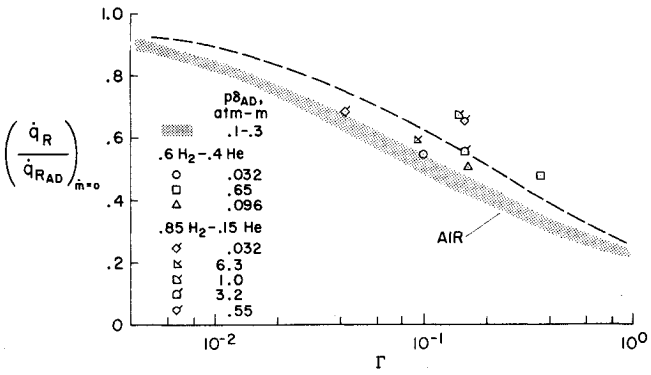


**Fig. 1 Calculated radiative cooling at stagnation point.**

Another mechanism which can reduce radiative heating of the body surface is the absorption of shock-layer radiation by ablation-product vapors. However, computing this effect is a difficult task which must be carried out with precision and a minimum of simplifying assumptions. For instance, calculations made for air show substantial differences in the fraction of incident radiation reaching the surface for similar flight conditions,[7,8] caused mainly by differences in the treatment of line radiation, viscosity, etc. Similarly, computations[9] of radiative heating reductions caused by ablation-product absorption in an atmosphere of 0.6 $H_2$ and 0.4 He showed an almost negligible attenuation during shallow angle entry. The calculations of Ref. 9 neglected the effect of molecular species in the ablation vapor and, judging by a trial calculation in air, this assumption was not expected to

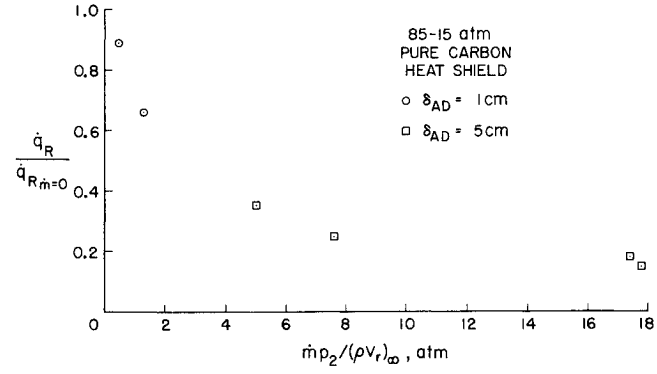


**Fig. 2 Calculated ablation vapor radiative blockage at stagnation point.**

**Table 2 Probes considered**

| | | | |
|---|---|---|---|
| Maximum radius, m | 0.55 | 0.80 | 1.08 |
| Entry mass, kg | 100 | 250 | 500 |

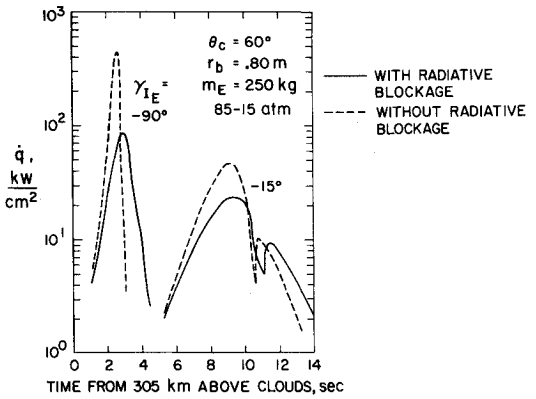


**Fig. 3 Heating pulses for steep and shallow entry angles.**

introduce large errors. However, at roughly the same time, calculations were being carried out to investigate the effect of ablation-product-radiation absorption during steep angle Jovian entry[10]; while all major ablation species were included, the fluid mechanics of the shock layer could not be treated realistically. However, a reduction by more than an order of magnitude was predicted.

To resolve this (seeming) discrepancy between the conclusions of Refs. 9 and 10, it was decided to incorporate the best current spectral details of the ablation vapors into Wilson's fluid-mechanical model and to investigate conditions representative of several entry angles. The results are shown in Fig. 2, where the ratio of the radiative-heating rate with ablation to that without is shown as a function of the product of the dimensionless ablation mass flux and shock-layer pressure. A pure carbon heat shield in an 0.85 $H_2$–0.15 He atmosphere was analyzed. Because the abscissa is dimensional, the grouping of terms used is probably incomplete; nonetheless, the trend is clearly evident. As the entry angle becomes steeper, the peak shock-layer pressure increases rapidly (while the dimensionless blowing rate decreases slowly) causing drastic reductions (up to 85%) in the fraction of radiative heating that reaches the body surface. The primary physical cause of the reduction is the increase in molecular number density, which is proportional to pressure, and which causes the gas to become opaque. Also, the ablation rates are sufficiently large that virtually none of this absorbed energy reaches the surface as convective heating.

The values shown in Fig. 2 were computed for a stagnation-point streamline. To the best of the authors' knowledge, there is no multidimensional method that has the necessary degree of sophistication to assure reasonable confidence in the results. As with radiative cooling, the stagnation-point

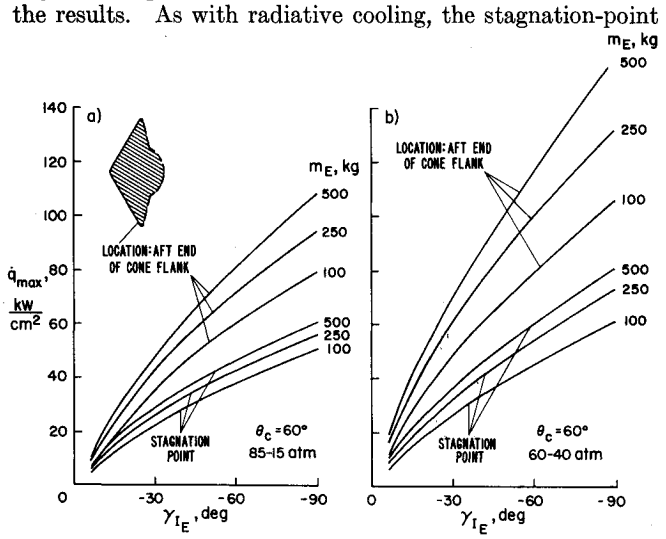


**Fig. 4 Maximum heating rates.**

absorption results were applied to the cone flank by assuming locally one-dimensional radiative transport from the shock to the body. This assumption may not be conservative since the residence time of ablation vapor may be shorter on the cone flank than at the stagnation point. Conversely, some conservatism must exist in the present approach since the influence of ablation vapors originating upstream is ignored; however, the rapid lateral spreading of the cone surface reduces the influence of upstream mass addition.

The "correlation" of Fig. 2 has, arbitrarily, been applied to the other atmospheres considered here as well.

### Convective Heating

In contrast to Ref. 1, it is assumed here that the boundary layer can be "blown off" by sufficiently massive ablation caused by radiative heating. This is substantiated by Wilson's calculations, which indicate no temperature gradient in the ablation layer near the wall. Also, in contrast to Ref. 1, for the majority of cases boundary-layer transition is assumed to start at a local Reynolds number of one million; fully turbulent flow is assumed at two million, with a straight-line variation of heat transfer in the transitional region. The effect of nose-roughness induced transition, beginning at Reynolds numbers as low as 20,000, also is considered.

The turbulent heat transfer was computed using the reference-enthalpy method for each atmosphere. The decreased effectiveness of mass addition in reducing turbulent convection was accounted for by using the one-third factor suggested in Ref. 11 and approximately supported by Ref. 12.

### Heat-Shield Response

The heat-shield response was calculated using the program of Ref. 13, which presumes thermodynamic equilibrium and includes conduction, reradiation and reflection, and mass-transfer blockage of convection and radiation. The thermodynamic properties of solid graphite and carbon vapor consisting of $C_1$–$C_5$ were taken from Ref. 14, while Ref. 15 was used for $C_6$–$C_{10}$ molecules. Heating rates computed in the absence of ablation were put into the program, as were Wilson's calculated radiative blockage values (Fig. 2). Surface recessions and material temperature histories were calculated. An outer layer of high-density graphite-like ablator (sp. gr. = 1.75) was assumed (to withstand the high shearing stresses and to minimize shape change) backed up by a low-density carbon felt insulator.

The results of the surface recession calculations from the transient ablation program greatly simplified subsequent heat shield calculations. First, since it was assumed that no particulate mass removal occurred, it was possible to use an approximate intrinsic heat of ablation of about 28 Mjoule/kg (12,000 Btu/lb), defined as the heat actually entering the heat shield per unit mass of material ablated. (The idea of a constant intrinsic heat of ablation depends on the assumption that sublimation is the dominant heat absorption mechanism and that processes such as reradiation do not play a major role. For the Jovian entries this assumption is generally good since the heating rates are very high, that is, much greater than the reradiation.) Second, because the total heating load was found to be fairly insensitive to entry angle, insulation requirements in subsequent calculations were assumed to be independent of entry angle. The insulation criterion used was that a shell, 0.5 cm thick, of high-density material remain after cessation of ablation, except in the immediate nose region where 1 cm was specified. This led to stipulation of a 2 cm layer of carbon felt insulator (sp. gr. = 0.1), with 2.5 cm being used in the nose region. (Several commercial low-density carbon felts were considered, and it was found that the lowest density material resulted in the lightest insulation weight and least back-face temperature rise.)

### Trajectory Calculations

The relation used for determining the flight path was basically the Allen-Eggers equation for ballistic entry.[16]‡ However, certain corrections had to be applied. For example, the ballistic coefficient varied with time; the rotation of the atmosphere with the planet had to be allowed for; and, where necessary, the flight-path angle was permitted to change during entry. The procedures for these corrections were as follows:

To the first order of accuracy, the changes in $m/C_DA$ are primarily caused by ablation which reduces $m$, while changes in $C_DA$ are small. Therefore, Eq. (5) of Ref. 1 was used to account for the changing ballistic coefficient during entry. For the computation of descent time, the vehicle's mass loss was integrated and subtracted from the entry mass at 20 values of the velocity. Both the velocity vector and the flight-path angle used in the Allen-Eggers equation were calculated with respect to the rotating atmosphere by assuming constant atmospheric rotation velocity over the altitude range of interest, which is small compared to the planet's radius. In presenting results, however, inertial coordinate flight-path angles are used. Last, for shallow flight-path angles, significant deviations from the entry value (assumed to be constant in the Allen-Eggers equation) can occur. For these entries the equations of motion were solved numerically, and either descent angles typical of the maximum heating period were used, or descent angles were varied with velocity.

## Results

Heating rates and heat-shield mass fractions have been calculated for direct atmospheric entry at low and high latitudes. Posigrade low-latitude entries are emphasized because they exploit the planet's high rotational rate. Attitude stabilization has been assumed so that angle of attack remains at or near zero during entry. An inertial reference entry velocity of 61.5 km/sec has been used. Inertial reference entry angles from $-6.3°$ to $-90°$ were considered; skip-out would occur at about $-2.5°$. The entry conditions were defined for an altitude of 305 km above the cloud top.

No provisions are made in the computations of heat-shield mass fractions for afterbody heat shielding, structural support for the heat shield, or factors of safety.

### Equatorial Region Entry

Shallow, posigrade, low-latitude entries permit lower $V_r$ and hence sharply reduced peak heating, surface pressures, and deceleration rates. For instance, for $\gamma_{IE} = -6.3°$, $V_r$ is about 49 km/sec; for $-30°$, 52 km/sec, while for $-90°$ it exceeds 60 km/sec. Moreover, as heating rates and pressures rise, the probability that forms of thermomechanical mass removal, other than sublimation, will occur increases,§ and it might prove necessary to limit entry angles if heat-protection capabilities are significantly reduced. There are no experimental facilities for testing materials at the peak heating rates experienced during Jupiter entry over most of the entry angle range.

### Heating Rates

The calculated heating rates at the aft flank station on a 60° half-angle cone are shown in Fig. 3, for the nominal weight body, for both steep ($-90°$) and shallow ($-15°$) entries. Rates are shown both with (solid lines) and without (dashed lines) radiative blockage by boundary-layer species to demonstrate the powerful influence of this effect. For the vertical entry, radiative blockage reduces the peak heating by a factor of 5, from 440 to 86 kw/cm²; even for the shallow entry, a factor of 2 decrease occurs, from 46 to 23.5 kw/cm². The shock-layer pressures at peak heating (with blockage) are about 30 atm for the vertical entry and about 6 atm for the shallow one. Note that even with radiative blockage, heating loads are large; the heating rates exceed 50 kw/cm² for about a second and 15 kw/cm² for about 2.5 sec for the steep and shallow entry, respectively. The second peak in the shallow-entry heating history results from boundary-layer transition to turbulence; for the vertical entry, transition is unimportant since massive ablation due to radiative heating blows the boundary layer off the surface. The difference in duration of the heating pulses with and without ablation vapor radiative blockage is due to the much more rapid mass loss of the body experiencing no radiative blockage, which causes these bodies to decelerate faster. (For the steep entry without blockage, about three-quarters of the entry mass is ablated making this example of only academic interest.) Unless otherwise specified, all subsequent results will include radiative blockage effects.

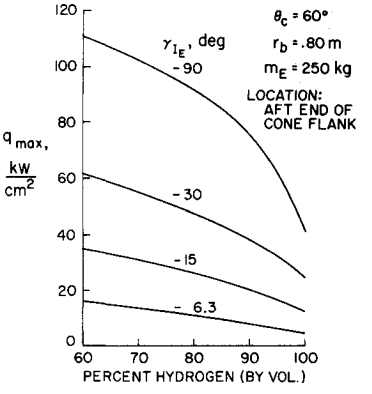


**Fig. 5 Effect of atmosphere on peak heating rates.**

The peak-heating rates experienced at the aft end of the 60° cone flanks and stagnation points are shown in Fig. 4 for all three bodies in the two hydrogen-helium atmospheres. As in Fig. 3 the maximum rates are entirely due to radiation. As the entry is steepened from $-6.3°$ to $-90°$, the maximum heating goes up by a factor of about 10. For the 85–15 atm (Fig. 4a), the cone flanks experience values to about 100 kw/cm² for steep entry, depending on body size and weight (ballistic coefficient). For the 60–40 atm (Fig. 4b) the rates are even greater, ranging up to 150 kw/cm². The (ablating) stagnation-point values are roughly half as large, mainly because the shock layer is much thinner at the stagnation point.

The decrease in peak heating caused by increasing the hydrogen content of the atmosphere is further emphasized in Fig. 5. Note that heating rates decrease monotonically with increasing hydrogen concentration; in pure hydrogen, the rates are about one-third as large as in the 60–40 atm.

### Heat Shielding Requirements

Two examples of temperature histories, for very shallow ($-6.3°$) and fairly steep ($-30°$) entry angles are shown in Fig. 6 at the aft end of the flank on a 60° half-angle cone. For both entry angles, the surface temperature rapidly rises to about 4500°K, while the temperature at the interface between the ablator and insulator climbs much more slowly to about 2750°K for the $-6.3°$ case and about 2100°K for

‡ The heating and trajectory calculations were stopped at 5 km/sec since the heating pulse was essentially over by then. Thus, one of the basic assumptions of the Allen-Eggers equations was satisfied in that the drag was still substantially greater than the weight component parallel to the flight path.

§ Although particulate removal is always undesirable, it is not necessarily intolerable. Particles in the ablation layer, or shock layer, can absorb (by vaporizing), block and scatter, radiative energy.

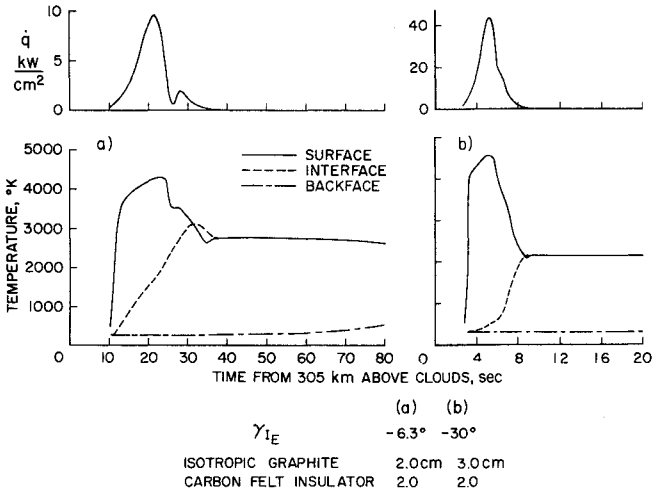


**Fig. 6 Ablator and insulator temperature histories. a) $\gamma_{I_E} = -6.3°$; b) $\gamma_{I_E} = -30°$.**

the −30° case. In contrast, the back face of the insulator stays almost at constant temperature during most of the period. Since the vehicle must decelerate to nearly sonic speed before the heat shield and insulation can be discarded, additional time is consumed, roughly equal to the time elapsed at the end of the heating period. Thus, heat conduction into the insulator continues and, if the period is long enough, causes a slow rise of back-face temperature. The surface recessions corresponding to the cases of Fig. 6 are shown in Fig. 7. The severity of the thermal environment is emphasized, especially for the steeper entry, where the recession rate approaches 1 cm/sec.

The reason for using a 60° cone half-angle is evident from Fig. 8, where the heat-shield mass fraction is shown as a function of cone half-angle. A 60° half-angle is close to minimizing heat-shield mass fractions for most entry angles, and will be referred to as "optimum," although heating rates are not minimized. Increasing the half-angle significantly beyond 60° would cause a fundamental change in the character of the shock layer from an essentially conical flowfield to a blunt-body one. The resulting increase in shock-layer thickness would enhance the radiative heating of much of the forebody without providing any significant increase in drag coefficient. (The total heat input is proportional to the ratio of heat-transfer coefficient to drag coefficient.[16])

In Fig. 9, a comparison is made between the mass-loss-fraction variation with entry angle for the two hydrogen-helium atmospheres, both with and without radiative blockage. The mass-loss ratios for the cases with radiative blockage are around 0.3, being similar for both atmospheres and almost independent of entry angle, for $\gamma_{IE} > -25°$. For contrast, the mass-loss cases without blockage rise rapidly with entry angle, peaking at about three-quarters of the initial mass for steep entry. (Note that a cone half-angle of 50° was used in the latter case, and is closer to

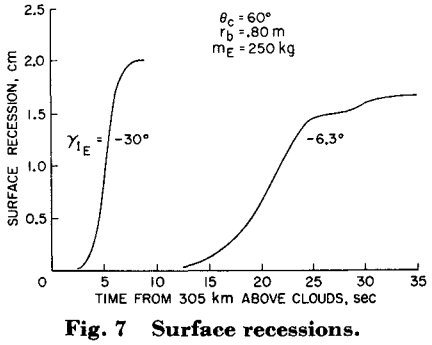


**Fig. 7 Surface recessions.**

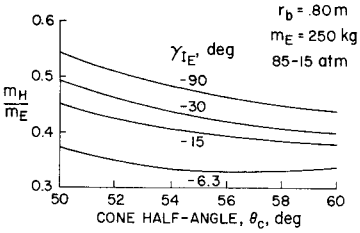


**Fig. 8 Variation of heat-shield mass fraction with cone half-angle.**

optimum for this condition.) Should experiments and more refined calculations fail to confirm large radiative blockage effects, entries may have to be limited to shallow angles.

The heat-shield mass fractions (accounting for radiative blockage) are presented in Fig. 10a for both hydrogen-helium atmospheres; all three bodies fall within narrow ranges for each atmosphere, and shaded bands are shown. For the 85–15 atm, the heat-shield fractions rise slowly with increasing entry angle from about 0.33 to 0.47: for the 60–40 atm, heat-shield fractions range from 0.40 to 0.44, with minimal entry-angle effect. Although the peak heating rates are roughly 40% higher in the 60–40 atm (Fig. 4), the lower scale height (which determines the duration of the heating pulse) offsets the higher rates, so that the total heating loads in the two atmospheres are similar. The analysis also has a tendency to equalize the heat input because the ablation vapor radiative blockage values from the 85–15 atm are used for the 60–40 atm as well.

The heat-shield mass fraction decreases monotonically with increasing hydrogen content of the atmosphere (Fig. 10b) except for steep entries, which appear to have broad maxima for hydrogen concentrations between 70% and 80%, depending on the fairing of the curves. Heat-shielding requirements are considerably less in pure hydrogen.

### Effect of Boundary-Layer Transition Reynolds Number

Boundary-layer transition to turbulence in the previous results was assumed to begin at a local Reynolds number of one million. Under these conditions convective heating had only a small influence on heat shielding. The possibility of large-scale surface roughness caused by very rapid, or irregular, ablation and high shearing stresses experienced during steep entry can raise doubts about achieving laminar flow to Reynolds numbers as high as one million. Therefore, the effect of transition at Reynolds numbers as low as 20,000 was investigated; fully turbulent flow was assumed to be established at 40,000.

A shallow entry (−6.3°) heating pulse, caused predominantly by radiation, is shown in Fig. 11. Transition that is assumed to start at a one-million Reynolds number will cause a second, much smaller pulse, which peaks at about 28 sec (solid line). However, if transition begins at a Reynolds number of 20,000, the heating is represented by the dashed line starting at 24 sec of elapsed time. The main

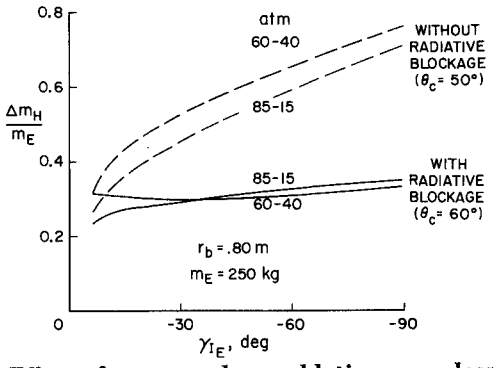


**Fig. 9 Effect of entry angle on ablation mass loss (with and without radiative blockage).**

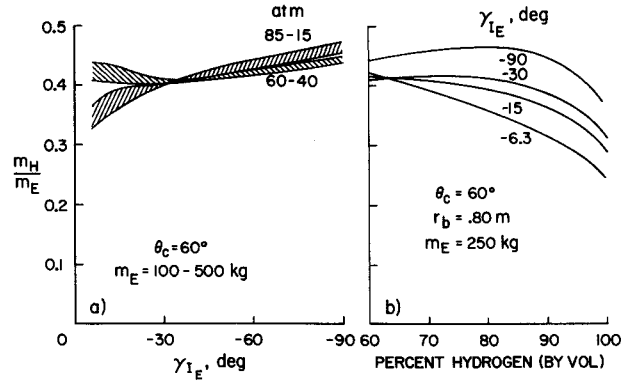


**Fig. 10 Variation of heat-shield mass fraction: a) with entry angle; b) with hydrogen concentration.**

heating pulse is almost unaffected by early transition because of powerful radiative heating that causes massive ablation which "blows" the boundary layer off the surface. Thus most of the additional convective heating occurs after radiative heating has ceased, resulting in about a 20% increase in heat-shield fraction for the shallow entry. Since radiative heating rises rapidly with increasing entry angle, the effect of early transition is lessened for steeper entries. For example, lowering transition Reynolds number again by a factor of 50 requires a 10% increase in heat-shield weight for $\gamma_{IE} = -15°$, while for steep entries the increases are negligible.

### Polar-Region Entry

At very high latitudes the planet's tangential velocity is small and does not significantly affect the vehicle's entry velocity with respect to the atmosphere. Since very steep entries are hardly affected by the planet's rotation, heating rates and heat-shield fractions should be similar to those for equatorial-region entry; however, shallow entries will experience greater relative entry velocities than before and heavier heat shields will be required.

The results of calculations for polar-entry conditions are shown in Fig. 12; the 60° cone half-angle is still nearly optimum over the whole range of entry angles. As expected, at the aft cone flank, the peak heating rates on shallow entry are about 50% higher than for similar equatorial entry; for steep entry the rates are comparable in both planetary regions (compare with Fig. 4). (Actually, the approach geometry precludes vertical entry at the poles.) The shallow-angle polar entries require drastic increases in heat shielding, while those for steep entry are similar to equatorial region cases. For instance, for entry into the 85–15 atm, at $\gamma_{IE} = -6.3°$ the heat-shield fraction approaches 0.55, for an increase of 63% over the equatorial case, while in the 60–40 atm the heat-shield fraction is nearly 0.54, representing a 28% increase. Note, however, that the heat-shield fractions decrease with increasing entry angle for the nearly constant

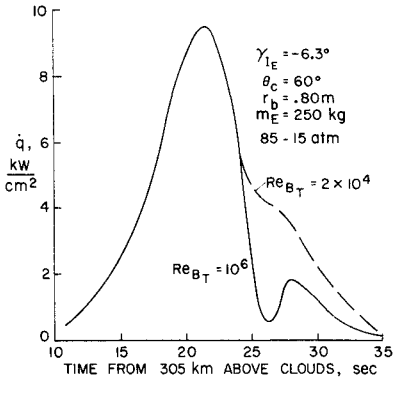


**Fig. 11 Effect of early transition on shallow entry heating pulse.**

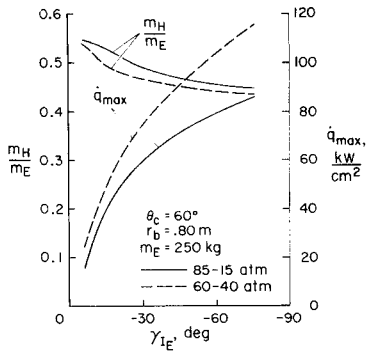


**Fig. 12 Peak heating rates and heat-shield fractions for polar-region entry.**

relative entry velocities experienced during polar region-entry, while for equatorial-region entries $V_r$ increases considerably with entry angle, causing the heat-shield fraction either to increase slowly or to remain relatively insensitive to entry angle, as shown in Fig. 10.

## Conclusions

The following tentative conclusions are based on this study of Jupiter atmospheric entry:

1) Ballistic entries of large half-angle cones (60°) may be feasible over the entire range of entry angles for posigrade equatorial entries with heat-shield mass fractions of the order of 0.45 of the mass at entry. For polar-region entries, heat-shield mass rises to about 0.55 of the entry mass. These mass fractions are based on the assumption that no mechanical erosion or spalling of the heat shield occurs.

2) Early boundary-layer transition does not appear to be a critical problem, since massive blowing caused by radiative heating appears capable of blocking the turbulent convection from reaching the wall most of the time.

3) For atmospheric compositions containing 60% or more hydrogen, peak heating rates will vary from about 10 kw/cm² for shallow up to about 150 kw/cm² for nearly vertical entry.

The preceding conclusions are critically dependent on verifying the assumptions made, and on extrapolations of present technology in several key areas:

1) The calculations of the extent to which ablation-product vapors can effectively block radiative heating need further refinement, extension to other atmospheric compositions and, especially, extension to multidimensional flowfields. Experimental verification of the calculations is very important.

2) Improved understanding of heat-shield material behavior at high heating rates is essential. The peak heating rates experienced even during shallow Jupiter entry exceed those of present technology. Experimental facilities capable of operating at high heating rates for sufficiently long durations are needed for testing candidate heat-shield materials.

3) A reliable measurement of the hydrogen/helium ratio of Jupiter's atmosphere is very important. A helium-rich atmosphere could make entries considerably more difficult than discussed herein.

## References

[1] Tauber, M. E., "Atmospheric Entry Into Jupiter," *Journal of Spacecraft and Rockets*, Vol. 6, No. 10, Oct. 1969, pp. 1103–1109.

[2] Owen, T. and Mason, H. P., "The Abundance of Hydrogen in the Atmosphere of Jupiter," *The Astrophysical Journal*, Vol. 154, Oct. 1968, pp. 317–326.

[3] Owen, T. and Mason, H. P., "New Studies of Jupiter's Atmosphere," *Journal of Atmospheric Sciences*, Vol. 26, No. 5, Sept. 1969, pp. 870–873.

[4] McElroy, M. B., "Atmospheric Composition of the Jovian Planets," *Journal of Atmospheric Sciences*, Vol. 26, No. 5, Sept. 1969, pp. 798–812.

[5] Page, W. A., Compton, D. L., Borucki, W. J., Ciffone, D. L., and Cooper, D. M., "Radiative Transport in Inviscid Nonadiabatic Stagnation-Region Shock Layers," *AIAA Progress in Astronautics and Aeronautics: Thermal Design Principles of Spacecraft and Entry Bodies*, Vol. 21, edited by J. T. Bevans, Academic Press, New York, 1969, pp. 75–114.

[6] Chin, J. H. and Hearne, L. E., "Shock-Layer Radiation for Sphere-Cones With Radiative Decay," *AIAA Journal*, Vol. 2, No. 7, July 1964, pp. 1345–1347.

[7] Coleman, W. D. et al., "Effects of Environmental and Ablator Performance Uncertainties on Heat-Shielding Requirements for Hyperbolic Entry Vehicles," *Journal of Spacecraft and Rockets*, Vol. 5, No. 11, Nov. 1968, pp. 1260–1270.

[8] Wilson, K. H., "Stagnation Point Analysis of Coupled Viscous-Radiating Flow With Massive Blowing," CR-1548, June 1970, NASA.

[9] Wilson, K. H., "Massive Blowing Effects on Viscous, Radiating Stagnation Point Flow," AIAA Paper 70-203, New York, 1970.

[10] Vulliet, W. G., Sand, S. J., and Findley, W. B., "Sputter Treatment of Ablation in the Atmosphere of Jupiter," Final Report, JPL Contract 952480, Gulf General Atomics, June 30, 1969.

[11] Adams, M. C., "Recent Advances in Ablation," *ARS Journal*, Vol. 29, No. 9, Sept. 1959, pp. 625–632.

[12] Canning, T. N., Tauber, M. E., and Wilkins, M. E., "Review of Recent Ballistic Range Boundary-Layer Transition Work on Ablating Bodies at Ames," *Proceedings—Boundary Layer Transition Study Group*, Aerospace Corp., San Bernardino, Calif., July 11 and 12, 1967.

[13] Moyer, C. B. and Rindal, R. A., "An Analysis of the Coupled Chemically Reacting Boundary Layer and Charring Ablator," Rept. 66-7, March 1967, Aerotherm Corp.

[14] *JANAF Thermochemical Tables*, The Dow Chemical Co., Aug. 1965.

[15] Duff, R. E. and Bauer, S. H., "The Equilibrium Composition of the C/H System at Elevated Temperatures," LA-2556, Sept. 1961, Los Alamos Scientific Lab.

[16] Allen, H. J. and Eggers, A. J., "A Study of the Motion and Aerodynamic Heating of Missiles Entering the Earth's Atmosphere at Supersonic Speeds," TN 4047, 1957, NACA.

JUNE 1971 J. SPACECRAFT VOL. 8, NO. 6

# Ablative Material Tests under Transient Heating Simulating Ballistic Re-Entry

BARRY J. MITCHEL*
*Avco Systems Division, Wilmington, Mass.*

**The ablative and insulative performance of reference silica phenolic and carbon phenolic heat shield materials was investigated under simulated trajectory heating characteristic of a medium-performance ballistic vehicle. A 10-Mw, 4-arc plasma-jet facility generated a stepwise-transient, supersonic, turbulent heating environment in a pipe specimen configuration. Agreement between experimental and theoretical values for surface and internal temperatures, surface recession, char depth, and weight loss was generally good for the silica phenolic, except during terminal heating when the melt removal rate was increased rapidly by aerodynamic shear stress. Agreement also was good for carbon phenolic with a 30° cloth layup, except near peak heating when carbon sublimation became the dominant ablative mechanism. However, the same material with a 90° layup was susceptible to mechanical erosion.**

## Nomenclature

$A$ = turbulent heating correlation factor
$C_2$ = second radiation constant = $2.59 \times 10^4$ $\mu$-°R
$c$ = specific heat
$g$ = force-mass conversion constant = 32.174 lbm-ft/sec$^2$-lbf
$H$ = total enthalpy
$\Delta H$ = enthalpy increase during reaction
$h$ = convective heat-transfer coefficient
$k$ = thermal conductivity
$M$ = Mach number
$m$ = sonic-throat mass flux
$q,q^*$ = heat flux and heat of ablation
$Re$ = Reynolds number
$r$ = radial distance
$S$ = heat-sink capacity at cooled surface
$St$ = Stanton number
$s$ = stoichiometric ratio for combustion
$T$ = temperature
$t$ = time
$U$ = gas flow speed
$V$ = flight speed
$v$ = surface or char-front speed
$w$ = weight
$W$ = mass fraction of oxygen in gas stream
$\alpha,\epsilon$ = absorptance and emittance
$\gamma$ = flight path angle
$\delta$ = char depth
$\eta$ = transpiration blocking coefficient
$\theta$ = cone half-angle
$\lambda$ = wavelength of radiation
$\nu$ = 0, 1, or 2 for slab, cylinder, or sphere
$\rho$ = material density
$\rho_g$ = change of density = $\rho_v - \rho_c$
$\sigma$ = Stefan-Boltzmann radiation constant = $0.476 \times 10^{-12}$ Btu/sec-ft$^2$-°R$^4$
$\tau$ = aerodynamic shear stress
$\Phi$ = transpiration-blocking function

### *Subscripts*

$A,a$ = ablation conditions, ambient conditions at cooled surface
$B$ = brightness
$C$ = cold-wall convective
$c,d$ = charred material and decomposition (charring) process
$E$ = re-entry altitude = 300 kft
$e,g$ = external gas stream and pyrolysis gas

Presented as Paper 69-150 at the AIAA 7th Aerospace Sciences Meeting, New York, January 20–22, 1969; submitted March 3, 1969; revision received January 15, 1971. This work was supported by Air Force Materials Laboratory, Air Force Systems Command through Contract AF33(615)-3923 under the technical guidance of R. W. Farmer (MANC). The author wishes to thank many associates, including H. E. Hoercher, P. J. Roy, F. L. Tempesta, and R. Shaw Jr.

* Senior Consulting Scientist, Hyperthermal Simulation and Instrumentation Section, Material Applications Department. Member AIAA.